



RESEARCH ARTICLE

How does land use/cover influence gully head retreat rates? An in-situ simulation experiment of rainfall and upstream inflow in the gullied loess region, China

Hongliang Kang¹  | Wenlong Wang^{1,2} | Mingming Guo³ | Jianming Li^{2,4}  | Qianhua Shi¹

¹State Key Laboratory of Soil Erosion and Dryland Farming on the Loess Plateau, Institute of Water and Soil Conservation, Northwest A&F University, Yangling, PR China

²Institute of Soil and Water Conservation, Chinese Academy of Sciences and Ministry of Water Resources, Yangling, PR China

³Key Laboratory of Mollisols Agroecology, Northeast Institute of Geography and Agroecology, Chinese Academy of Sciences, Harbin, PR China

⁴Department of Soil and Water Conservation, Yangtze River Scientific Research Institute, Wuhan, PR China

Correspondence

Wenlong Wang, State Key Laboratory of Soil Erosion and Dryland Farming on the Loess Plateau, Institute of Water and Soil Conservation, Northwest A&F University, Yangling, Shanxi 712100, PR China.
Email: nwafu_wwl@163.com

Funding information

National Natural Science Foundation of China, Grant/Award Number: 42077079 and 41571275; China Postdoctoral Science Foundation, Grant/Award Number: 2020M681062

Abstract

Land use/cover plays a crucial role in gully head retreat (GHR). However, little is known about how land use/cover influences GHR rates. An in situ simulation experiment of rainfall and upstream inflow was conducted in a gullied loess region to investigate hydraulic erosion, mass movements, and linear GHR processes under three types of land use/cover (bare land, grassland, and shrub-grass land). The results showed that the average linear GHR rates on grassland and shrub-grass land were 87–89% and 72–81% lower than that on bare land ($0.99\text{--}2.06\text{ cm min}^{-1}$), respectively. Gully heads retreat by hydraulic and gravitational erosion. In the case of hydraulic erosion, upstream runoff incision is dominant on bare land, while undercutting by on-wall and jet flow dominates on grassland and shrub-grass land. In the case of mass movement, collapse dominates with a frequency of 62–100%, of which gully sidewall collapse is most common, especially on bare land and it acts to widen the gully. Gully headwall collapse dominates on grassland and shrub-grass land to cause retreat of the gully head. Overall, on bare land, upstream runoff incision dominates GHR. However, on grassland/shrub-grass land GHR is mainly driven by the undercutting of on-wall and jet flow and subsequent gully headwall collapses. As a consequence, the GHR length on bare land exponentially increases over time, while on grassland or shrub-grass land, it discretely increases as an analogous step function. Moreover, the average linear GHR rate on grassland was considerably lower than that on shrub-grass land, implying that an optimized vegetation restoration pattern enhances GHR control.

KEYWORDS

collapse, gully head retreat, hydraulic erosion, land use/cover, mass movement, simulated rainfall

1 | INTRODUCTION

Gully erosion, a serious issue that is widespread worldwide, has long been recognized as an important research topic for soil erosion research (Bennett & Wells, 2019; Castillo & Gómez, 2016). Gully erosion has on-site effects such as crop yield loss (Valentin, Poesen, &

Li, 2005), landscape dissection, and potentially the transformation of countryside into badland (Makanzu Imwangana, Dewitte, Ntombi, & Moeyersons, 2014). Furthermore, gully erosion is an important source of sediments and therefore has off-site impacts such as raising riverbeds (stream siltation), which causes flooding and water pollution (Poesen, Nachtergaele, Verstraeten, & Valentin, 2003). Vast efforts

have been made globally to prevent or counter gully erosion in recent years (Addisie et al., 2017; Frankl et al., 2016; Yan et al., 2020; Zegeye et al., 2017). Gully head retreat (GHR), as the major process of gully initiation and development (Guan et al., 2021; Poesen, Torri, & Vanwallegem, 2011; Vanmaercke et al., 2016; Zheng, Xu, & Qin, 2016), needs to be controlled. Therefore, it is of great value to reveal the processes and mechanisms of GHR.

A gully head is normally a vertical or near-vertical drop or discontinuity from an upstream area to a gully bed (Hanson, Robinson, & Cook, 1997, 2001). Globally, GHR rates vary with a large range of 0.01–135 m yr⁻¹ in length, 0.01–3268 m² yr⁻¹ in area and 0.002–47430 m³ yr⁻¹ in volume (Vanmaercke et al., 2016). The rates are affected by various factors such as the size and shape of the upstream area draining to the gully head, weather, and climatic conditions, land use/cover and soil characteristics, topography, vegetation, seismicity, etc. (Vanmaercke et al., 2016). Rainfall and the drainage area are the two most important impacting factors causing variations in GHR rates at local and global scale (Beer & Johnson, 1963; Rieke-Zapp & Nichols, 2011; Thompson, 1964; Vanmaercke et al., 2016). Furthermore, soil physicochemical properties determine the susceptibility of gully heads to concentrated flow scouring and seepage and subsequent piping and thereby significantly affect GHR rates (Faulkner, 1995; Kariminejad, Hosseinalizadeh, Pourghasemi, Bernatek-Jakiel, & Alinejad, 2019; Oostwoud Wijdenes, Poesen, Vandekerckhove, & Ghesquiere, 2000; Vandekerckhove, Poesen, Oostwoud Wijdenes, & Gysels, 2001; Vanwallegem, Poesen, Nachtergaele, & Verstraeten, 2005). Moreover, land use/cover, generally involves various vegetation cover conditions, soil properties, and management policies and may directly affect GHR.

Initially, land use/cover influences hydraulic and topographic conditions for gully initiation (Faulkner, 1995; Hayas, Poesen, & Vanwallegem, 2017; Poesen et al., 2003; Samani, Chen, Khalighi, Wasson, & Rahdari, 2016; Torri et al., 2018; Vandekerckhove et al., 2000). Land uses, such as forested areas, rangelands, pastures and cropland, have clear effects on the resistance of a site to gully head development (Torri et al., 2018; Torri & Poesen, 2014). Vandekerckhove et al. (2000) showed that vegetation type and cover could better explain differences in topographical threshold levels for gully initiation than could climate conditions in Mediterranean Europe. Likewise, Hosseinalizadeh et al. (2019) confirmed that land use had the greatest influence on gully headcut occurrence in the loess area of Golestan Province, Iran. Accordingly, land use/cover can play a key role in gully initiation.

Land use/cover affects GHR rates. From a temporal perspective, changes in land use/cover over time influence gully erosion and/or GHR rates for the same individual gullies or study sites. Vandekerckhove, Poesen, & Govers (2003) identified the importance of land use changes according to considerable differences between GHR rates measured for individual gullies over short- and medium-term scales. Mukai (2017) reported that the temporal variation in land use/cover was strongly correlated with the rates of gully erosion in Ethiopia based on photogrammetric techniques. It has even been concluded that land use change was expected to have a greater impact

than climate change on gully erosion (Valentin et al., 2005). Some land use changes, for instance the destruction of extensive shrubland and conversion to apricot orchards (Faulkner, 1995), removal of indigenous vegetation (Tebebu et al., 2010), enlargement of arable fields (Nachtergaele & Poesen, 1999), soil compaction, road construction, and urbanization (Carvalho Junior et al., 2010), will decrease gully incision thresholds, increase runoff generation, and subsequently lead to a significant increase in gully erosion risk and rates (Poesen et al., 2003). In contrast, land use rationalization may play an important role in controlling gully development. Bork, Li, Zhao, Zhang, & Yang (2001) confirmed that an increase in forest area and/or decrease in cropland area in the upper region of the Yangtze River (SW China) in the second half of the 20th century significantly alleviated gully development. However, Martínez-Casasnovas, Ramos, & García-Hernández (2009) found that land/vegetation cover on gully walls did not affect sidewall retreat and mass movement in the period of 1975–2002 in a gully head of the Penedès region (northeastern Spain).

From a spatial perspective, GHR rates vary under different land-use/cover types over the same period. Oostwoud Wijdenes et al. (2000) reported that the maximum number of active gully heads and the highest gully activity were found on farmland planted with apricot, intercropped with wheat, and on abandoned land and grassy fields in southeastern Spain. Li, Zhang, Zhu, He, & Yao (2015) suggested that gully areas increased more quickly in catchments where the proportion of farmland was greater than 15% and in catchments dominated by grassland than in catchments dominated by forestland on the Chinese Loess Plateau. Fan et al. (2004) found that gully heads on bare land retreated at the highest rate they measured - 146.7 cm yr⁻¹, followed by that on farmland (30.0–86.3 cm yr⁻¹), grassland (29.3 cm yr⁻¹), and forestland (5.0–16.7 cm yr⁻¹) in the Yanmou Basin of southwestern China. In the same basin, Wang, Zhong, Liu, & Li (2008) found that GHR rates for different land use/cover types showed a decreasing order as follows: bare land, farmland for only crops, mixture of orchards and crops, combination of forest and grass and combination of forest, shrubs, and grass. Nevertheless, Vanwallegem et al. (2005) observed almost identical frequencies of deep (1.7 ± 0.8 m) gully occurrences on fallow land, maize field and wheat land in the loess region of Belgium and concluded that land use was not a decisive factor in the formation of deep gullies. Similarly, Mukai (2017) concluded that land use/cover over a similar period played a minor role in the area-specific volume of the gully networks.

Overall, land use/cover change plays a dominant role in the initiation of gullies and has been widely reported to affect GHR rates. Evidently, land use/cover not only influences soil properties to determine the soil erosion sensitivity to gully erosion but also affects runoff production to determine erosive force causing gully initiation and development (Mhired et al., 2019; Nyssen et al., 2006; Tebebu et al., 2010; Vanmaercke et al., 2016). To date, little is known about how land use/cover affects GHR rates. Since the difficulties associated with accurately quantifying the effects of land use/cover on runoff production and soil properties, land use/cover-related parameters have rarely

been included in GHR prediction models (Allen, Arnold, Auguste, White, & Dunbar, 2018; Li et al., 2015; Vanmaercke et al., 2016). Furthermore, processes controlling GHR include runoff incision, plunge pool erosion by jet flow, scour hole erosion by on-wall flow, fluting, piping and seepage, mass failure, and sediment transportation (Bradford, Piest, & Spomer, 1978; Chen et al., 2013; Dong et al., 2019; Morgan & Mngomezulu, 2003; Qin, He, Zheng, Han, & Zeng, 2018; Stein, Julien, & Alonso, 1993; Vanmaercke et al., 2016; X. M. Xu, Wilson, Zheng, & Tang, 2020); however, the process that becomes dominant under each land use/cover type is still unclear. Therefore, we undertook a series of in-situ simulations of rainfall and upslope runoff on the gullied loess region of China to: (a) investigate the effects of land use/cover (i.e., bare land, grassland and shrub-grass land) on hydraulic erosion and mass movement during GHR; (b) identify the difference in the linear GHR processes among the three different land use/cover types from the perspectives of hydraulic erosion and mass movement; and (c) reveal the influence mechanism of land use/cover on the linear GHR rate.

2 | MATERIALS AND METHODS

2.1 | Study area

The study was carried out at the Xifeng Soil and Water Conservation Experimental Station, a field station operated by the Yellow River Conservancy Commission (YRCC) of the Ministry of Water Resources, China. The station is located within the Nanxiaohegou watershed (E107°30′-107°37′, N35°41′-35°44′), which is a typical catchment of the gullied loess region in the Loess Plateau (Figure 1). The watershed is located near of the Pu River, covering an area of 36.5 km² and an altitude of 1050 m-1423 m. The watershed is within the arid and

semiarid climate zone with a mean annual precipitation of 552.1 mm, of which 55.2% occurs during July–September. The dominant soil type is loess-loam. The mean annual sediment transport modulus was 4350 t km⁻², more than 85% of which came from gully erosion during 1955–1974 in the watershed (Liu, Liu, & Yang, 2014). The Nanxiaohegou watershed has been a testing region for comprehensive and scientific control of soil and water loss in the Loess Plateau since the establishment of the Xifeng Soil and Water Conservation Experimental Station in 1951. Land use/cover in the watershed has been greatly improved and gully erosion has been well controlled through 50 years of management (R. J. Zhang et al., 2015). The main plants in the region include evergreen trees such as *Pinus tabulaeformis* Carr. and *Platycladus orientalis* (L.) Franco, deciduous trees such as *Robinia pseudoacacia* L. and *Armeniaca sibirica* (L.) Lam., shrubs such as *Ziziphus jujuba* Mill. var. *spinosa* (Bunge) Hu ex H.F. Chow. and *Hippophae rhamnoides* L. and grasses such as *Medicago sativa* L., *Bothriochloa ischaemum* (L.) Keng, *Setaria viridis* (L.) Beauv., *Agropyron cristatum* (L.) Gaertn. and *Artemisia vestita* Wall. ex Bess.

2.2 | Experimental design

2.2.1 | Experimental treatments

Nine experimental runs (three land use/cover type treatments and three slope gradient treatments) were carried out. Three typical land use/cover types were chosen in the study area, including bare land, grassland, and shrub-grass land. The slope gradients of upstream discharge areas in the field are mostly less than 10° (Yang, Li, Wang, & Yang, 2014); hence, 3°, 6°, and 9° were chosen under each land use/cover type. Each run was conducted under the same experimental duration, rainfall intensity, and inflow discharge.

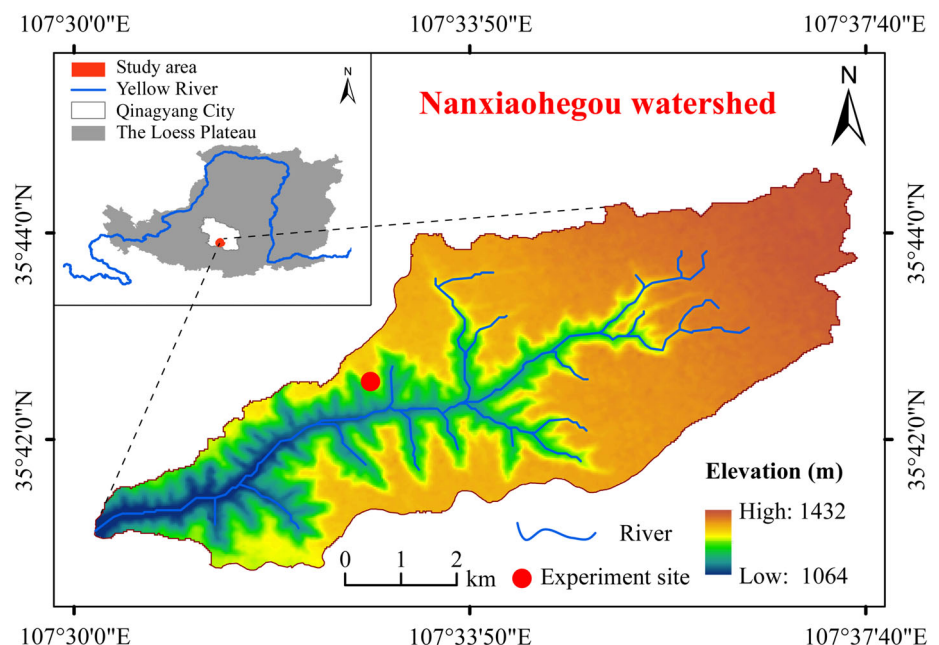


FIGURE 1 Locations of the study area and experiment site [Colour figure can be viewed at [wileyonlinelibrary.com](https://onlinelibrary.com)]

2.2.2 | Experimental duration, rainfall intensity, and inflow discharge design

GHR is driven mostly by rainstorms in the study region. In the Xifeng region, more than 70% of the rainstorms have a short duration of less than 180 min (H. X. Zhang, 1983). To observe a well-developed gully head under the experimental condition, the duration of the simulated rainfall was set to 180 min. Based on the standard of heavy rain in the Loess Plateau proposed by H. X. Zhang (1983), a 180-min rainstorm typically has a rainfall intensity of more than 22.8 mm hr⁻¹. As a consequence, in this study, a rainfall intensity of 30-mm hr⁻¹ was selected. The experimental inflow discharge was calculated using the following formula (Guo et al., 2019):

$$q = \frac{\lambda \times A \times i \times d}{D}, \quad (1)$$

Where: q is the inflow discharge, m³hr⁻¹; A is the upstream area, km², with a range of 0.145–8.696 km² (Che, 2012); D is the width of the upstream area, km; i is the rainfall intensity, $i = 30$ mm hr⁻¹; d is the plot width, $d = 1.5$ m in this study; and λ is the runoff coefficient on tableland in this study region, $\lambda = 0.2$ (Xing, Li, Liu, Jia, & Liu, 1991). The inflow discharge was calculated to be in a range of 8.42–35.85 m³ hr⁻¹ with a mean of approximately 16.22 m³ hr⁻¹ (Table S1). As a result, the inflow discharge was set to 16 m³ hr⁻¹. Table 1 shows the basic information about the experimental design.

2.3 | Experimental plot preparation

The experimental site was at the Xifeng Soil and Water Conservation Experiment Station, facilitating clear water and an electricity supply. Three flat bench terraces were chosen and used as bare land, grassland, and shrub-grass land (Figure 2a). Basic information about the main vegetation types and coverage, soil properties, and root biomass density of the three types of lands is shown in Table 2. Three experimental plots were built on each terrace (Figure 2b), and a total of nine experimental plots were established. Each plot consisted of an upstream slope, gully headwall, and gully bed (Figure 2c). The widths, depths, and slopes of the gully heads were set to 1.5, 1.2 m, and 90°, respectively (Guo et al., 2019). The horizontal lengths of the upstream slopes and the gully beds were set to 8.0 and 1.0 m, respectively, and

the widths were both set to 1.5 m (Figure 2d). The slope gradient of the gully bed was set to be the same as that of the upstream slope. All plots were built from April to May 2015. First, the gully headwalls and gully beds were built through soil excavation. Then, slope-cutting technology was applied to construct the upstream slopes. The above-ground vegetation on the constructed upstream slopes was destroyed, therefore, the plots were left for 1 year of natural restoration to allow the aboveground vegetation to grow.

2.4 | Experimental installations

Experimental installations included rainfall simulation equipment, flow release setups, sampling pools, and photographic devices are shown in Figure 2d. A rainfall simulator installed 2.05 m above the soil surface was formed from a rectangular framework of PVC pipes with 20 sprinkling nozzles each with a radius of 1.0 mm (Xu, Liu, et al., 2015; Xu, Zhang, Wang, Zhao, & Yan, 2015). The nozzles were evenly arranged with spacing intervals of 0.67 m. Valves and pressure gauges were installed in the water-supply pipe to adjust and monitor the rainfall intensity. The measurements before the experiment indicated that the simulated rainfall could reach the target intensity with a uniformity of more than 80%. Flow release setups were composed of: a 20 m³ cistern, submersible pumps, tee-joints, water pipes with a diameter of 65 mm, and a steady flow tank (length × width × height: 0.6 m × 1.5 m × 0.5 m). Likewise, valves and a split electromagnetic flowmeter (GY-LED), with an accuracy of 0.01 m³ hr⁻¹, were used to adjust and monitor the inflow discharge. The sampling pool was used to gather runoff and sediment discharged from the experimental plot. Photographic devices, including a high-definition webcam, Logitech C920 PRO with a resolution of 2.0 megapixels and a tripod, were installed in front of the plot to record the erosion processes.

2.5 | Experimental procedure

The experiment was conducted from July to September 2016. Unfortunately, the plot on the grassland under an upstream slope gradient of 9° was destroyed in a rain storm in August 2015 because of the development of an undetected cave under the upstream area. Before the experiment, the aboveground parts of the grass and shrubs was cut to maintain the same height (i.e., 5 cm) to clearly observe the

TABLE 1 Experimental treatments

Land use/cover type treatments	Upstream slope gradient treatments (°)	Run code	Simulated rainfall intensity (mm hr ⁻¹)	Inflow discharge (m ³ hr ⁻¹)	Experimental duration of each run (min)
Bare land	3, 6, 9	Run 1, 2, 3	30	16	180
Grassland	3, 6, 9	Run 4, 5, 6			
Shrub-grass land	3, 6, 9	Run 7, 8, 9			

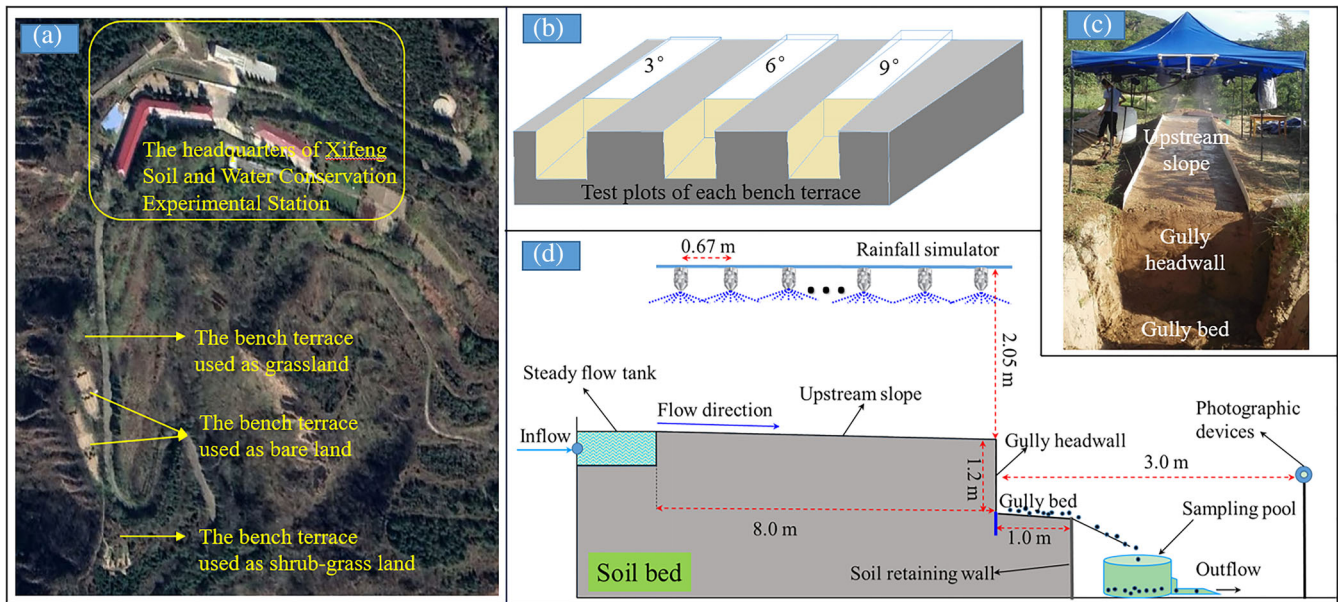


FIGURE 2 (a) The locations of the three bench terraces used as bare land, grassland, and shrub-grass land; (b) the three test plots built on each bench terrace; (c) the components of each experimental plot; and (d) a sketch of the plot and the experimental setups [Colour figure can be viewed at [wileyonlinelibrary.com](https://onlinelibrary.wiley.com)]

morphology of the gully head and flow velocity. The height was greater than the runoff depth so that the plants still acted with resistance to runoff. Additionally, to ensure an almost equivalent initial moisture in all plots before the experiment, simulated rainfall with an intensity of $<15 \text{ mm hr}^{-1}$ was applied to each plot. Specifically, each plot was subjected to the simulated rainfall until surface runoff was generated and then was allowed to stand for 24 hr covered with evaporation-preventive plastic sheeting. According to the hydrological process under natural conditions, simulated rainfall with an intensity of 30 mm hr^{-1} was applied first, and at the time, runoff was generated, water from the steady flow tank was released at a rate of $16.0 \text{ m}^3 \text{ hr}^{-1}$. The released water was uniformly distributed across the width of each plot at the beginning of each run. When the mixture of released water and rainfall runoff flowed to the outlet of the plots, we started monitoring and collecting measurements (Figure S1).

2.6 | Experimental monitoring and measurements

2.6.1 | Linear retreat processes

Headcuts migrate in different ways (Gardner, 1983; Holland & Pickup, 1976; Stein & Julien, 1993). Unlike previous studies (Su et al., 2014; Zhang, Xiong, Zhang, Zhang, et al., 2018), we identified the retreat lengths of different parts of the gully headwall rather than the average retreat length of the gully head. In this study, we defined the GHR length (*GL*), headwall retreat length (*WL*), and headwall scour hole depth (*HD*). The *GL* was defined as the maximum distance between the retreated gully headwall and the originally built gully headwall from the top plan view (Figure 3). If the upper part of

the gully headwall retreated faster than the lower part, only the *GL* was measured (Figure 3a). A critical cross-section of 929 cm^2 was chosen to distinguish the retreated gully from the developed rills on the eroded upstream slope (Oostwoud Wijdenes, Poesen, Vandekerckhove, Nachtergaele, & De Baerdemaeker, 1999; Poesen, Vandaele, & Van Wesemael, 1996). However, if the lower part of the gully headwall retreated faster than the upper part, a scour hole (Collison, 2001; Guo et al., 2019; Zhang, Xiong, Zhang, Wu, et al., 2018) formed on the headwall; in this case, the *HD* was defined as the distance from the deepest point to the opening plane of the scour hole (Figure 3b). Additionally, the *WL* was defined as the distance from the deepest point of the headwall scour hole to the originally built gully headwall (Figure 3b). A steel ruler with an accuracy of 1 mm was used to measure the above indicators at a 5-min interval.

2.6.2 | Hydraulic parameters and mass movement process

Runoff discharge was monitored with a standard runoff tank. Flow velocity, flow surface width, and flow depth in the upstream discharge area were manually measured. Flow velocity was measured by the color tracer method using potassium permanganate solution and a stopwatch. All measurements were repeated every 5 min.

Mass movement generally occurred occasionally and suddenly; therefore, video image capture technology was used to obtain information on each mass movement event, such as the occurrence time, position (e.g., gully headwall and gully sidewall), and type (e.g., collapse, slide, and mudflow), as well as the resulting morphology changes from mass movements.

TABLE 2 Basic information about the three types of land use/cover

Land use/cover type	Soil property				Root biomass density in different diameter classification (kg m ⁻³)					
	Dominant vegetation type	Vegetation coverage (%)	Bulk density (g cm ⁻³)	Infiltration rate (mm hr ⁻¹)	Disintegration rate (g min ⁻¹)	>0.25 mm aggregates content (%)	≥2 mm	1–2 mm	0.5–1 mm	≤0.5 mm
Bare land	No vegetation	0	1.32 ± 0.10	26.36 ± 1.07	2.05 ± 0.00	38.29 ± 0.12	0	0	0	0
Grassland	Crested wheatgrass	60–66	1.31 ± 0.03	33.93 ± 2.21	0.54 ± 0.11	62.84 ± 3.86	0.69 ± 0.06	0.43 ± 0.01	0.26 ± 0.07	0.38 ± 0.02
Shrub-grass land	Wild jujube; Alfalfa	78–84	1.25 ± 0.03	42.13 ± 2.00	0.74 ± 0.05	52.23 ± 0.38	1.13 ± 0.11	0.47 ± 0.13	0.17 ± 0.05	0.22 ± 0.02

Note: Wild jujube (*Ziziphus jujuba* Mill. var. *spinosa* (Bunge) Hu ex H.F. Chow.); Alfalfa (*Medicago sativa* L.).

2.7 | Data analysis

Hydraulic parameters including the shear stress (τ , Pa), stream power (ω , w m⁻²), and unit stream power (U , m s⁻¹) were calculated as follows:

$$\tau = \rho_w \cdot g \cdot R \cdot J \quad (2)$$

$$\omega = \rho_w \cdot g \cdot R \cdot J \cdot v = \tau \cdot v \quad (3)$$

$$U = v \cdot J, \quad (4)$$

where R is the hydraulic radius, m; v is the flow velocity, m s⁻¹; g is the acceleration due to gravity, m s⁻²; ρ_w is the water density, kg m⁻³; and J is the hydraulic gradient, m m⁻¹.

All statistical analyses and figures were carried out with SPSS 21.0 and ORIGIN 8.5 software. Nonlinear regression analyses were used to determine the statistical relationships between stream power, GHR length, headwall retreat length, and time duration. One-way analysis of variance was used to test for differences among the different experimental treatments.

3 | RESULTS

3.1 | Hydraulic erosion characteristics

3.1.1 | Runoff characteristics

Table 3 shows the averages of the runoff discharge and hydraulic parameters on the upstream slope. The average runoff discharge on bare land (14.06–14.75 m³ hr⁻¹ under upstream slope gradients of 3°–9°) was greater than that on grassland and shrub-grass land. Shrub-grass land, with the highest infiltration rate among the three types of land use/cover (Table 2), had the lowest runoff discharge (10.21–12.42 m³ hr⁻¹). Land use/cover change not only influenced the runoff discharge but also the hydraulic conditions on the upstream slope. In terms of the runoff velocity, as illustrated in Table 3, the average runoff velocity on the upstream slope for bare land (0.50–0.68 m s⁻¹) was 35–45% and 43–61% greater than for grassland and shrub-grass land, respectively. From the perspective of runoff energy, bare land had the greatest shear stress, stream power, and unit stream power on the upstream slope, which were 44–72%, 46–93%, and 50–75% higher than those on grassland and 28–104%, 57–90%, and 50–75% higher than those on shrub-grass land.

3.1.2 | Hydraulic erosion processes

Figure 4 shows the typical hydraulic erosion processes under the three types of land use/cover. On bare land, an incised channel first formed at the upper edge of the headwall driven by upstream runoff, which in turn further concentrated the runoff to incise the gully head (Figure 4a). Subsequently, the splashing point of the jet flow on the

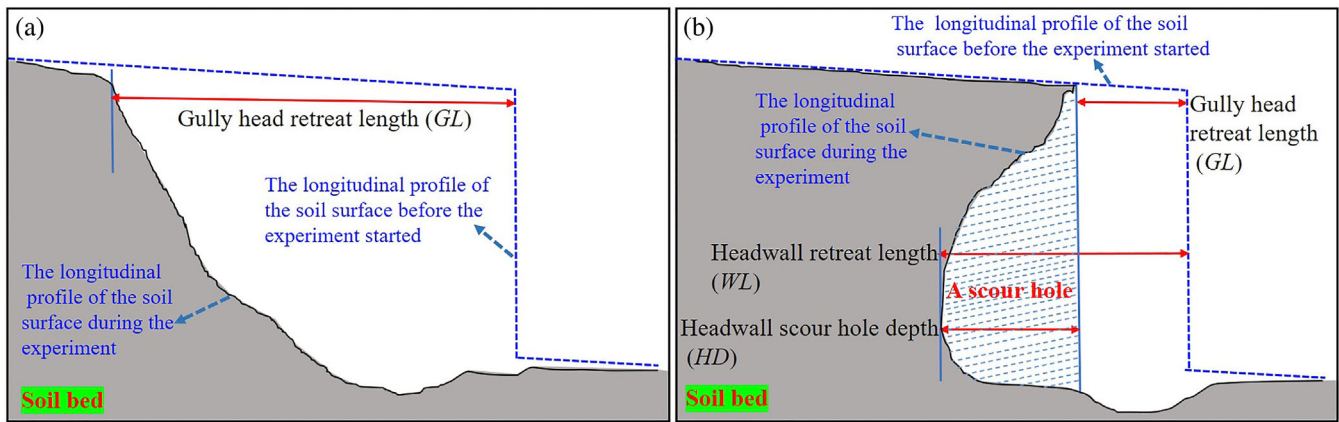


FIGURE 3 The longitudinal profiles of two typical retreated gully heads including (a) the upper part of the gully headwall retreating faster than the lower part and (b) the lower part of the gully headwall retreating faster than the upper part [Colour figure can be viewed at wileyonlinelibrary.com]

TABLE 3 The averages of inflow discharge, runoff discharge and hydraulic parameters on the upstream slope

Land use/cover type	Upstream slope gradient (°)	Inflow discharge (m ³ hr ⁻¹)	Runoff discharge (m ³ hr ⁻¹)	Runoff velocity (cm s ⁻¹)	Shear stress (N m ⁻²)	Stream power (W m ⁻²)	Unit stream power (m s ⁻¹)
Bare land	3	15.96	14.06	0.50	6.59	2.94	0.03
	6	16.08	14.27	0.61	8.50	4.65	0.07
	9	16.10	14.75	0.68	12.37	6.21	0.09
Grassland	3	15.97	10.98	0.37	3.82	2.02	0.02
	6	15.88	11.77	0.42	5.90	2.41	0.04
	9	—	—	—	—	—	—
Shrub-grass land	3	16.15	10.21	0.35	3.23	1.78	0.02
	6	16.11	11.26	0.38	6.63	2.45	0.04
	9	15.90	12.42	0.45	9.29	3.95	0.06

Note: —, The data on grassland under an upstream slope gradient of 9° failed to be obtained.

gully bed advanced with the retreat of the upper headwall; therefore, no obvious scour hole formed on the gully headwall or plunge pool on the gully bed. Therefore, upstream runoff incision dominated hydraulic erosion during GHR on bare land; as a consequence, the upper part of the gully headwall retreated faster than the lower part. However, on grassland and shrub-grass land, the upstream slope was slightly eroded with no obvious morphological change (Figure 4b,c). Furthermore, on-wall flow and jet flow seriously eroded the lower part of the gully headwall and the gully bed to form a scour hole and a plunge pool, respectively, and subsequently, the upper part of the gully headwall was hung (Figure 4b,c). Therefore, undercutting by on-wall and jet flow scour dominated hydraulic erosion during GHR on grassland and shrub-grass land, resulting in the faster retreat of the lower part of the gully headwall.

3.2 | Mass movement characteristics

Collapse, slide, mudflow, and topple were observed during GHR (Figure S2), of which collapse was dominant in mass movements

with a proportion of 62–100% of the total number of mass movement occurrences (Table 4). The proportion of collapse was the greatest on shrub-grass land, followed by that on grassland and bare land. Based on the occurrence position, collapse was divided into two types: gully headwall collapse and gully sidewall collapse. On bare land, gully sidewall collapse was the main type of collapse, while gully headwall collapse was dominant on grassland and shrub-grass land (Table 4). Furthermore, according to the gully morphological change resulting from the collapse events, gully headwall collapse was grouped into gully headwall scour hole collapse (GHSC), which enlarged the headwall scour hole (Figure 5a), and gully headwall overhanging mass collapse (GHOC), which directly led to linear GHR (Figure 5b); additionally, gully sidewall collapse was grouped into gully sidewall scour hole collapse (GSSC), which enlarged the sidewall scour hole (Figure 5c), and gully sidewall overhanging mass collapse (GSOC), which directly widened the gully (Figure 5d). On bare land, no GHOC but 5–10 occurrences of GSOC were observed, indicating that collapse played a very limited role in linear GHR for bare land but was critical to gully widening. However, on grassland and shrub-grass land, the 2–15 occurrences of



FIGURE 4 Gully head retreat processes driven by hydraulic erosion over time under different land use/cover types [Colour figure can be viewed at wileyonlinelibrary.com]

TABLE 4 The number of different types of mass movement occurrences

Land use/cover type	Upstream slope gradient (°)	Total number of mass movement occurrences	Mass movement type							Proportion of collapses to the total number of mass movement occurrences (%)
			Collapse							
			Gully headwall collapse		Gully sidewall collapse			Slide	Mudflow	
GHSC	GHOC	GSSC	GSOC							
Bare land	3	23	0	0	11	5	3	3	1	70
	6	21	0	0	8	5	1	3	4	62
	9	33	0	0	17	10	1	2	3	82
Grassland	3	17	8	2	2	2	0	3	0	82
	6	14	4	3	2	2	0	3	0	79
	9	—	—	—	—	—	—	—	—	—
Shrub-grass land	3	18	8	3	2	5	0	0	0	100
	6	28	5	11	3	8	0	1	0	96
	9	45	10	15	7	10	0	3	0	93

Note: GHSC, GHOC, GSSC, and GSOC represent gully headwall scour hole collapse, gully headwall overhanging mass collapse, gully sidewall scour hole collapse, and gully sidewall overhanging mass collapse, respectively. —, The data on grassland under an upstream slope gradient of 9° were not obtained.

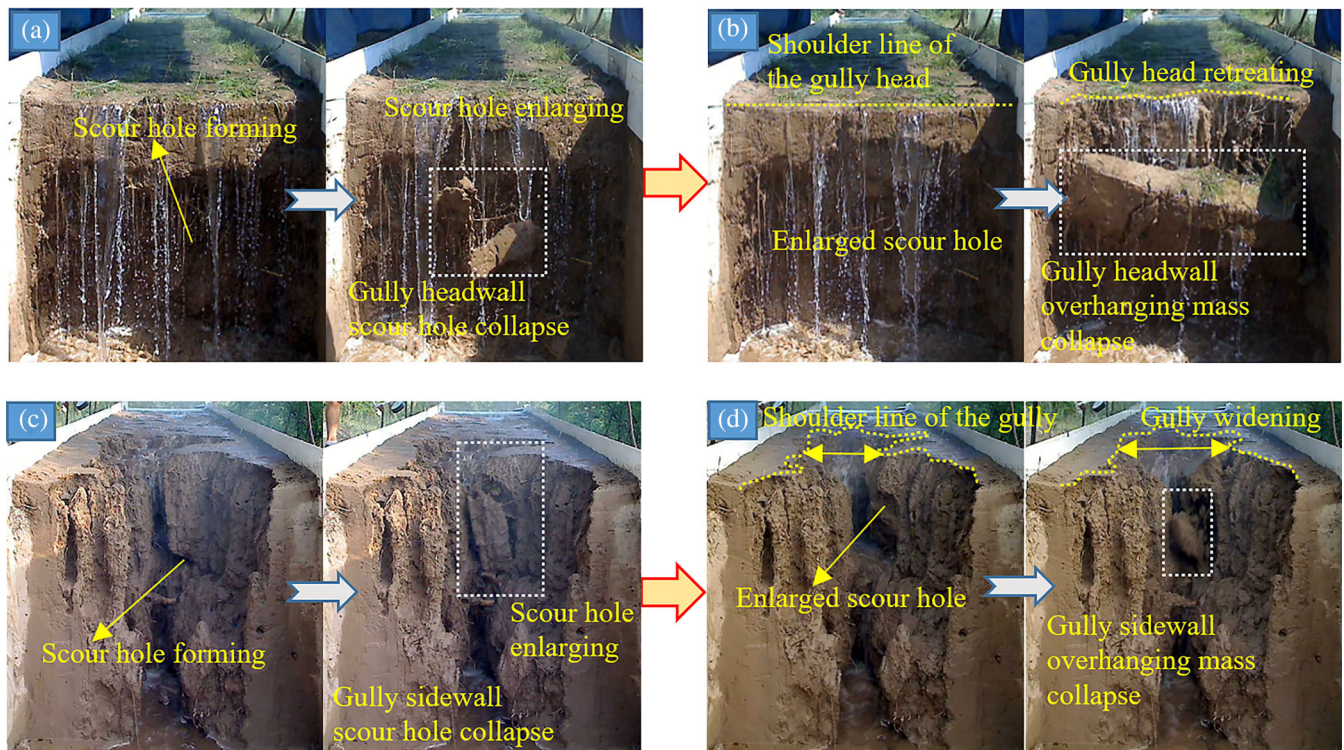


FIGURE 5 Collapse types including (a) gully headwall scour hole collapse, (b) gully headwall overhanging mass collapse, (c) gully sidewall scour hole collapse, and (d) gully sidewall overhanging mass collapse [Colour figure can be viewed at wileyonlinelibrary.com]

GHOC implied that collapse played a crucial role in linear GHR for grassland and shrub-grass land. Additionally, more GHOCs occurred on shrub-grass land than on grassland (Table 4).

3.3 | Linear GHR characteristics

3.3.1 | GHR length

The *GL* on bare land increased due to upstream runoff incision, while the *GL* on grassland and shrub-grass land increased due to gully headwall overhanging mass collapse. The *GL* on bare land increased exponentially as the retreat rate decreased over time (Figure 6a). However, the *GL* on grassland and shrub-grass land discretely increased as analogous step functions, of which the number of discrete increases in the *GL* on shrub-grass land was higher than that on grassland (Figure 6b,c). The decreased retreat rate over time on bare land was related to the decrease in upstream runoff energy over time (Figure S3). Bare land had the maximum total *GL* (177.8–369.6 cm), followed by that of shrub-grass land and grassland (Table 5). The average linear GHR rates on grassland and shrub-grass land were 87–89% and 72–81% lower than that (0.99–2.06 cm min⁻¹) on bare land, respectively. (Table 5). Additionally, the average linear GHR rate on shrub-grass land was

1.08–1.29-times greater than that on grassland under upstream slope gradients of 3°–6°.

3.3.2 | Gully headwall retreat length and headwall scour hole depth

The headwall scour hole formed only on grassland and shrub-grass land (Figure 4b,c). The *WL* was driven by on-wall flow and jet flow scour and increased as an exponential function over time. Shrub-grass land showed a faster temporal change than grassland (Figure 7a–c), with a lower runoff discharge (Table 3), indicating that the gully headwall on shrub-grass land was more sensitive to water erosion. The average retreat rates of the gully headwall on shrub-grass land were 28 and 22% greater than those on grassland under the upstream slope gradients of 3° and 6°, respectively (Table 5). The *HD* on grassland and shrub-grass land initially increased due to on-wall flow and jet flow scour and then suddenly decreased due to gully headwall overhanging mass collapse; afterward, it varied in a cyclic tendency of slowly increasing and abruptly decreasing (Figure 7d–f). Additionally, the number of abrupt decreases in the *HD* on shrub-grass land was higher than that on grassland. The maximum *HD* on grassland was greater than that on shrub-grass land (Table 5), indicating that the headwall overhanging mass collapsed on grassland with a deeper

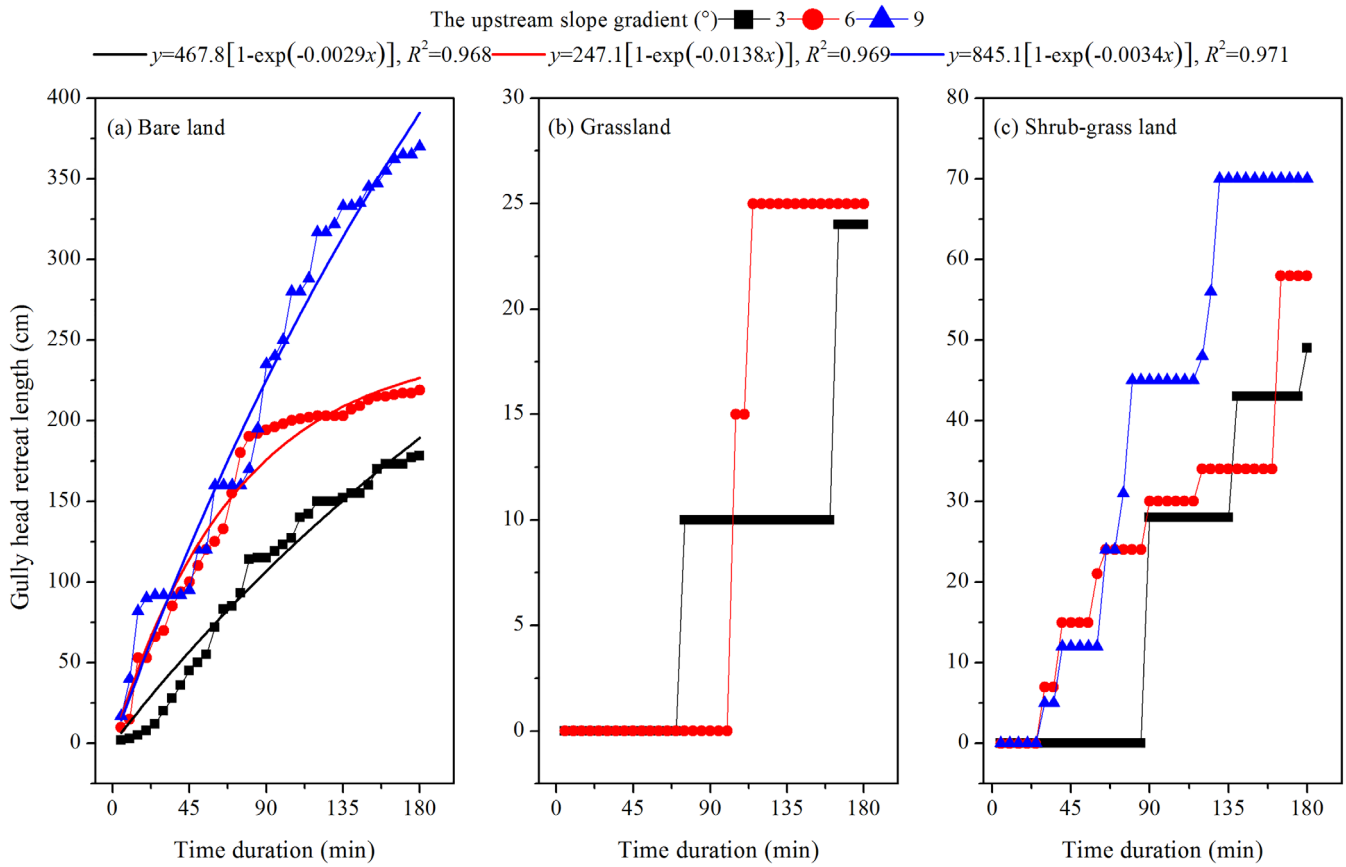


FIGURE 6 Temporal variation in the gully head retreat length (GL) under different upstream slope gradients [Colour figure can be viewed at wileyonlinelibrary.com]

TABLE 5 Characteristics of gully head retreat length, gully headwall retreat length, and headwall scour hole depth

Land use/cover type	Upstream slope gradient (°)	Gully head			Gully headwall		Headwall scour hole
		Total retreat length (cm)	Average linear retreat rate (cm min ⁻¹)	Amplitude of variation compared with bare land (%)	Total retreat length (cm)	Average linear retreat rate (cm min ⁻¹)	Maximum of headwall scour hole depth (cm)
Bare land	3	177.8	0.99				
	6	219.3	1.22				
	9	369.6	2.06				
Grassland	3	23.5	0.13	-87	64.9	0.36	51.9
	6	24.4	0.14	-89	59.2	0.33	40.5
	9	—	—	—	—	—	—
Shrub-grass land	3	49.0	0.27	-72	83.2	0.46	44.5
	6	58.2	0.32	-73	72.0	0.40	34.1
	9	70.3	0.39	-81	82.7	0.46	22.8

Note: The data on grassland under an upstream slope gradient of 9° were not obtained. —, There were no data for the gully headwall retreat and headwall scour hole depth on bare land.

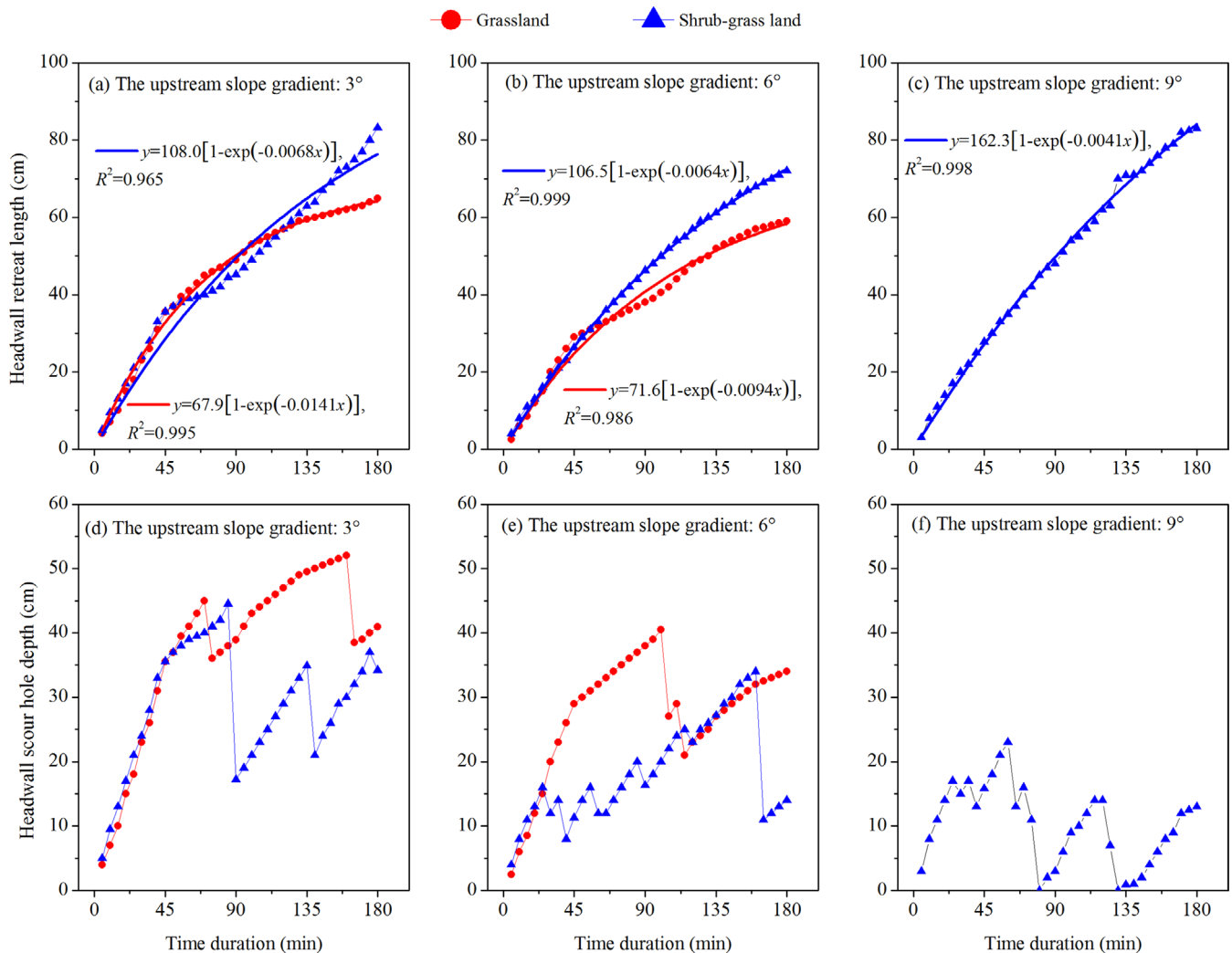


FIGURE 7 Temporal variations in (a–c) the gully headwall retreat length (*WL*) and (d–f) the headwall scour hole depth (*HD*) for different land use/cover types [Colour figure can be viewed at [wileyonlinelibrary.com](https://onlinelibrary.wiley.com)]

scour hole. This result further supports the conclusion that the headwall overhanging mass was more sensitive to collapse on shrub-grass land than it was on grassland.

4 | DISCUSSION

4.1 | Effects of land use/cover on hydraulic erosion processes

Our results showed that in the hydraulic erosion processes, upstream runoff incision was dominant on bare land, while undercutting by on-wall and jet flow dominated on grassland and shrub-grass land. Similar results on bare land and grassland were reported by Guo et al. (2019) for the Loess Plateau. However, the result on bare land in our study differed with the findings of previous studies undertaken in other places on bare soils (Chen et al., 2013; Robinson & Hanson, 1996). Consistent with Guo et al. (2019), upstream runoff incision, jet flow

and on-wall flow scour were observed to be the main hydraulic erosion processes in a gully head system subjected to rainfall and concentrated flow. These hydraulic erosion processes contributed in various degrees to GHR (Vanmaercke et al., 2016), which depended on the interaction of hydraulic stress and topsoil erodibility on the upstream slope, gully headwall, and gully bed (Collison, 2001; Moore, 1997; Stein & Julien, 1993; Temple & Moore, 1997). On bare land in our study and Guo et al. (2019), the loessal topsoil on the upstream slope was prone to concentrated flow (Knapen, Poesen, Govers, Gysels, & Nachtergaele, 2007); as a result, the upper headwall was eroded away through the upstream runoff incision. However, in Robinson & Hanson (1996), the bare upstream slope had a no- or little-erosion soil surface and an erodible sublayer. Likewise, the gully head in Chen et al. (2013) had a top layer of dry red soil, which was resistant to concentrated flow erosion (Knapen et al., 2007), and a bottom sandy layer, which was relatively erodible. Therefore, the upstream runoff incision was restricted in their studies, and undercutting of on-wall flow and jet flow scour dominated hydraulic erosion. On grassland

and shrub-grass land in our study, the upstream runoff could not incise the upstream slope because of the lower runoff discharge, velocity, and energy (Table 3) and increased soil resistance resulting from the existence of a dense root system, which enhanced the shear strength of the surface soil layer (Vannoppen, Vanmaercke, Baets, & Poesen, 2015). Furthermore, on-wall flow and jet flow eroded the lower part of the gully headwall and the gully bed, where sparse or no roots were distributed, to form a scour hole and a plunge pool (Guo et al., 2019).

4.2 | Effects of land use/cover on mass movement processes

In our study, collapses were dominant in mass movements, which is similar to the result found on steep loess slopes in Xu, Liu, et al. (2015). On bare land, collapse played a very limited role in linear GHR but was critical to gully widening; however, on grassland or shrub-grass land, collapse played a crucial role in linear GHR. The results are consistent with the findings of Guo et al. (2019). Additionally, similar to the conclusions proposed by several previous studies (Bradford et al., 1978; Dong et al., 2019; Guo et al., 2019; Istanbuluoglu, Bras, Flores-Cervantes, & Tucker, 2005; Robinson & Hanson, 1996), collapse of gully walls can suddenly increase GHR rates and contribute to the headward growth and widening of many gully systems. The role of collapse on linear GHR under different land use/cover was closely correlated to the topography of the gully head resulting from the main hydraulic erosion processes. In our present study, on bare land, upstream runoff incised the upstream slope to form a new sidewall and channel bed (Oostwoud Wijdenes & Bryan, 2001), and subsequent toe scour freed the hanging soil material on the sidewall (Figure 4a), which accelerated sidewall collapse. Therefore, collapse on bare land mainly widened the gully. However, on grassland and shrub-grass land, on-wall flow and jet flow undercut the gully headwall and freed the hanging soil material on the headwall, which accelerated headwall collapse under those types of land use/cover. Additionally, gully heads on grassland or shrub-grass land retreated much slower than those on bare land, resulting in the slower development of gully sidewalls (Figure 4); as a result, fewer sidewall collapses occurred. Therefore, collapse on grassland and shrub-grass land played a crucial role in the linear GHR.

In our experiment, more gully headwall overhanging collapses occurred on shrub-grass land than on grassland, and the headwall overhanging mass collapsed on grassland with a deeper scour hole than that on shrub-grass land. Similar to the observations by Robinson & Hanson (1996), the headwall overhanging mass collapsed when the headwall scour hole reached a critical shape resulting from a period of hydraulic erosion, in which the block weight exceeded the strength of the root-soil composition (Rengers & Tucker, 2014). Supported by Baets et al. (2008), the results in our study indicated that grassland had a higher strength and bank stability of the root-soil composition than did shrub-grass land. The effect of plant roots on gully bank stability is itself a 'double-edged sword' (Simon &

Collison, 2002; Yu, Zhang, Zhang, & Pei, 2012). On-the-one-hand, plants strengthen the soil strength through root reinforcement to stabilize slopes. On-the-other-hand, the root system can improve soil permeability to accelerate infiltration, resulting in the destabilization of gully banks. Overall, the gully stabilization effect of vegetation varies over a wide range, varying with the plant species, management practices (Bastola, Dialynas, Bras, Noto, & Istanbuluoglu, 2018) and some other conditions such as moisture and tension crack (Pollen, 2007; Zegeye, Langendoen, Steenhuis, Mekuria, & Tilahun, 2020). The results in our study may be attributed to the following causes. First, there was higher soil moisture in shrub-grass land during the test resulting from a higher infiltration rate (Table 2), which led to weaker soil strength than that on grassland. Second, the higher biomass density of the fine roots (<2 mm in diameter) and fibrous root system on grassland dominated by crested wheatgrass (Table 2) provided greater additional cohesion and enhanced gully bank stability (Zegeye et al., 2018). However, wild jujube and alfalfa on shrub-grass land have tap root systems, which provide lower additional cohesion. Finally, the root wedging of the large roots (>2 mm in diameter) and the distribution of many ant holes on shrub-grass land (Figure S4) increased the concentrated flow deeper into the gully head to increase the pore water pressure and weakened the soil strength (Simon & Collison, 2002).

4.3 | Effects of land use/cover on the linear GHR rate

The average linear GHR rate on grassland and shrub-grass land decreased by 87–89% and 72–81%, respectively, compared to that on bare land, implying that grasses and/or shrubs could strongly help control GHR. This result is in accordance with the findings of several previous studies (Fan et al., 2004; Guo et al., 2019; Li, Zhang, et al., 2015; Wang et al., 2008). Land use/cover with vegetation can reduce runoff discharge and greatly decrease runoff energy on upstream slopes of a gully head (Table 3). Additionally, soil covered by vegetation had much lower disintegration rates and much higher contents of water-stable aggregates (Table 2), which increased soil resistance to water erosion. Due to the above cases, upstream runoff incision was well controlled on vegetation-covered soils. However, only vegetation covering the upstream slope was insufficient to protect a gully head from retreating (Zegeye et al., 2020). According to our results, toe protection, such as planting and stone barrier on the toe of gully bank, should be applied to control undercutting from on-wall flow and jet flow scour (Zegeye et al., 2020).

The average linear GHR rate on shrub-grass land was much greater than that on grassland in our study, which resulted from the gully headwall on shrub-grass land being more sensitive to water erosion and the headwall overhanging mass being more sensitive to collapse than those on grassland. A similar conclusion was proposed in the same study area by Guo, Wang, Kang, and Yang (2018), who found that grassland dominated by *Cleistogenes caespitosa* Keng and *Artemisia sacrorum* Ledeb. showed lower soil erodibility of gully heads

than did shrubland and woodland. However, our finding is in contrast to the result reported in the Yanmou basin of southwestern China by Fan et al. (2004), who concluded that shrub-grass land had a lower GHR rate than grassland. This difference might be due to the different plant species on shrub-grass land and soil textures. The dominant plant on shrub-grass land was alfalfa in our study, which has a tap root system, collocating with the shrub wild jujube, which has a weaker controlling effect on linear GHR. Evidently, most studies have concluded that fibrous root systems have a more significant resistance to rill and gully erosion (Burylo, Rey, Mathys, & Dutoit, 2012; Li, Yu, et al., 2015; Vannoppen et al., 2015; Zegeye et al., 2018). Overall, land use/cover with different plant cover could have a very different effective control on GHR (Fan et al., 2004), and grass with fibrous root systems, such as crested wheatgrass, might be a better choice. Furthermore, according to the results from Fan et al. (2004) and vegetation configurations for controlling soil erosion in the Loess Plateau, grasses with fibrous root systems collocating with shrubs with deep root systems might be an optimal choice for controlling GHR.

5 | CONCLUSIONS

Land use/cover change not only plays a dominant role in the initiation of gullies but also affects GHR rates. However, little research has focused on how land use/cover affects GHR rates. This study sought to investigate the effects of land use/cover on hydraulic erosion processes, mass movement and linear GHR processes to reveal how land use/cover influences the linear GHR rate under an in situ rainfall and upslope runoff simulation experiment. Gully heads on bare land and grassland/shrub-grass land retreated in different ways because the main hydraulic process and mass movement type during GHR varied. On bare land, upstream runoff incisions were dominant processes in GHR, and gully sidewall collapse was dominant in the mass movements that widened the gully, whereas undercutting by on-wall and jet flow and subsequent gully headwall collapse dominantly led to GHR on grassland and shrub-grass land. Vegetation controlled the linear GHR well. However, land use/cover with different plant cover could have a very different control effectiveness on GHR. The gully headwall was more sensitive to water erosion and gully headwall overhanging mass collapse on shrub-grass land than on grassland, which explains why the gully head retreated faster on shrub-grass land than on grassland from hydraulic and gravitational aspects. Furthermore, plants with fibrous root systems have a better controlling effectiveness on GHR than plants with tap root systems. The optimal vegetation restoration pattern for GHR control should be further studied.

ACKNOWLEDGMENTS

This work was financially supported by the National Natural Science Foundation of China [grant numbers 42077079, 41571275] and the China Postdoctoral Science Foundation [2020M681062]. The authors would like to express deep gratitude to Dr. Pengfei Li for the suggestions and revising the article.

CONFLICT OF INTEREST

The authors declare no conflict of interest.

DATA AVAILABILITY STATEMENT

The data that support the findings of this study are available from the corresponding author upon reasonable request.

ORCID

Hongliang Kang  <https://orcid.org/0000-0001-6161-5250>

Jianming Li  <https://orcid.org/0000-0001-5888-7351>

REFERENCES

- Addisie, M. B., Ayele, G. K., Gessess, A. A., Tilahun, S. A., Zegeye, A. D., Moges, M. M., ... Steenhuis, T. S. (2017). Gully head retreat in the sub-humid Ethiopian Highlands: The Ene-Chilala catchment. *Land Degradation & Development*, 28, 1579–1588. <https://doi.org/10.1002/ldr.2688>
- Allen, P. M., Arnold, J. G., Auguste, L., White, J., & Dunbar, J. (2018). Application of a simple headcut advance model for gullies. *Earth Surface Processes and Landforms*, 43, 202–217. <https://doi.org/10.1002/esp.4233>
- Baets, S. D., Poesen, J., Reubens, B., Wemans, K., Baerdemaeker, J. D., & Muys, B. (2008). Root tensile strength and root distribution of typical Mediterranean plant species and their contribution to soil shear strength. *Plant and Soil*, 305, 207–226. <https://doi.org/10.1007/s11104-008-9553-0>
- Bastola, S., Dyalynas, Y. G., Bras, R. L., Noto, L. V., & Istanbuluoglu, E. (2018). The role of vegetation on gully erosion stabilization at a severely degraded landscape: A case study from Calhoun Experimental Critical Zone Observatory. *Geomorphology*, 308, 25–39. <https://doi.org/10.1016/j.geomorph.2017.12.032>
- Beer, C. E., & Johnson, H. P. (1963). Factors in gully growth in the deep loess area of Western Iowa. *Transactions of the ASAE*, 6, 237–240. <https://doi.org/10.13031/2013.40877>
- Bennett, S. J., & Wells, R. R. (2019). Gully erosion processes, disciplinary fragmentation, and technological innovation. *Earth Surface Processes and Landforms*, 44, 46–53. <https://doi.org/10.1002/esp.4522>
- Bork, H., Li, Y., Zhao, Y. T., Zhang, J. H., & Yang, S. Q. (2001). Land use changes and gully development in the Upper Yangtze River basin, SW-China. *Journal of Mountain Science*, 19, 97–103. <https://doi.org/10.3969/j.issn.1008-2786.2001.02.001>
- Bradford, J. M., Piest, R. F., & Spomer, R. G. (1978). Failure sequence of gully headwalls in Western Iowa. *Soil Science Society of America Journal*, 42, 323–328. <https://doi.org/10.2136/sssaj1978.03615995004200020025x>
- Burylo, M., Rey, F., Mathys, N., & Dutoit, T. (2012). Plant root traits affecting the resistance of soils to concentrated flow erosion. *Earth Surface Processes and Landforms*, 37, 1463–1470. <https://doi.org/10.1002/esp.3248>
- Carvalho Junior, O., Guimaraes, R., Freitas, L., Gomes-Loebmann, D., Gomes, R. A., Martins, E., & Montgomery, D. R. (2010). Urbanization impacts upon catchment hydrology and gully development using multi-temporal digital elevation data analysis. *Earth Surface Processes and Landforms*, 35, 611–617. <https://doi.org/10.1002/esp.1917>
- Castillo, C., & Gómez, J. A. (2016). A century of gully erosion research: Urgency, complexity and study approaches. *Earth-Science Reviews*, 160, 300–319. <https://doi.org/10.1016/j.earscirev.2016.07.009>
- Che, X. L. (2012). *Study of distribution characteristic and evolution of headward erosion on Dongzhi tableland of the loess gully region* (pp. 66–67). Yangling, China: Northwest A&F University (in Chinese).
- Chen, A. Q., Zhang, D., Peng, H., Fan, J. R., Xiong, D. H., & Liu, G. C. (2013). Experimental study on the development of collapse of

- overhanging layers of gully in Yuanmou Valley, China. *Catena*, 109, 177–185. <https://doi.org/10.1016/j.catena.2013.04.002>
- Collison, A. J. C. (2001). The cycle of instability: Stress release and fissure flow as controls on gully head retreat. *Hydrological Processes*, 15, 3–12. <https://doi.org/10.1002/hyp.150>
- Dong, Y. F., Xiong, D. H., Su, Z. A., Duan, X. W., Lu, X. N., Zhang, S., & Yuan, Y. (2019). The influences of mass failure on the erosion and hydraulic processes of gully headcuts based on an in situ scouring experiment in a dry-hot valley of China. *Catena*, 176, 14–25. <https://doi.org/10.1016/j.catena.2019.01.004>
- Fan, J. R., Liu, X. Z., Zhou, C. B., Wang, X. D., Zhu, H. Y., & Zhu, B. (2004). Impacts of LUCC on gully erosion in Yuanmou basin of Jinshajiang arid-hot valley. *Journal of Soil and Water Conservation*, 130–132, 18. <https://doi.org/10.13870/j.cnki.stbcb.2004.02.033> (in Chinese).
- Faulkner, H. (1995). Gully erosion associated with the expansion of unterraced almond cultivation in the coastal Sierra de Lujar, S. Spain. *Land Degradation & Development*, 6, 179–200. <https://doi.org/10.1002/ldr.3400060306>
- Frankl, A., Deckers, J., Moulaert, L., Van Damme, A., Haile, M., Poesen, J., & Nyssen, J. (2016). Integrated solutions for combating gully erosion in areas prone to soil piping: Innovations from the drylands of Northern Ethiopia. *Land Degradation & Development*, 27, 1797–1804. <https://doi.org/10.1002/ldr.2301>
- Gardner, T. W. (1983). Experimental study of knickpoint and longitudinal profile evolution in cohesive, homogeneous material. *Geological Society of America Bulletin*, 94, 572–664. [https://doi.org/10.1130/0016-7606\(1983\)94<664:ESOKAL>2.0.CO;2](https://doi.org/10.1130/0016-7606(1983)94<664:ESOKAL>2.0.CO;2)
- Guan, Y. B., Yang, S. T., Zhao, C. S., Luo, H. Z., Chen, K., Zhang, C. B., & Wu, B. W. (2021). Monitoring long-term gully erosion and topographic thresholds in the marginal zone of the Chinese Loess Plateau. *Soil and Tillage Research*, 205, 104800. <https://doi.org/10.1016/j.still.2020.104800>
- Guo, M. M., Wang, W. L., Kang, H. L., & Yang, B. (2018). Changes in soil properties and erodibility of gully heads induced by vegetation restoration on the Loess Plateau, China. *Journal of Arid Land*, 10, 712–725. <https://doi.org/10.1007/s40333-018-0121-z>
- Guo, M. M., Wang, W. L., Shi, Q. H., Chen, T. D., Kang, H. L., & Li, J. M. (2019). An experimental study on the effects of grass root density on gully headcut erosion in the gully region of China's Loess Plateau. *Land Degradation & Development*, 30, 2107–2125. <https://doi.org/10.1002/ldr.3404>
- Hanson, G. J., Robinson, K. M., & Cook, K. R. (1997). Headcut migration analysis of a compacted soil. *Transactions of the ASAE*, 40, 355–361. <https://doi.org/10.13031/2013.21280>
- Hanson, G. J., Robinson, K. M., & Cook, K. R. (2001). Prediction of headcut migration using a deterministic approach. *Transactions of the ASAE*, 44, 525–531. <https://doi.org/10.13031/2013.6112>
- Hayas, A., Poesen, J., & Vanwalleghem, T. (2017). Rainfall and vegetation effects on temporal variation of topographic thresholds for gully initiation in Mediterranean cropland and olive groves. *Land Degradation & Development*, 28, 2540–2552. <https://doi.org/10.1002/ldr.2805>
- Holland, W. N., & Pickup, G. (1976). Flume study of knickpoint development in stratified sediment. *Geological Society of America Bulletin*, 87, 76–82. [https://doi.org/10.1130/0016-7606\(1976\)87<76:FSOKDI>2.0.CO;2](https://doi.org/10.1130/0016-7606(1976)87<76:FSOKDI>2.0.CO;2)
- Hosseinalizadeh, M., Kariminejad, N., Chen, W., Pourghasemi, H. R., Alinejad, M., Mohammadian Behbahani, A., & Tiefenbacher, J. P. (2019). Gully headcut susceptibility modeling using functional trees, naïve Bayes tree, and random forest models. *Geoderma*, 342, 1–11. <https://doi.org/10.1016/j.geoderma.2019.01.050>
- Istanbulluoglu, E., Bras, R. L., Flores-Cervantes, H., & Tucker, G. E. (2005). Implications of bank failures and fluvial erosion for gully development: Field observations and modeling. *Journal of Geophysical Research: Earth Surface*, 110, F01014. <https://doi.org/10.1029/2004JF000145>
- Kariminejad, N., Hosseinalizadeh, M., Pourghasemi, H. R., Bernatek-Jakiel, A., & Alinejad, M. (2019). Gis-based susceptibility assessment of the occurrence of gully headcuts and pipe collapses in a semiarid environment: Golestan Province, NE Iran. *Land Degradation & Development*, 30, 2211–2225. <https://doi.org/10.1002/ldr.3397>
- Knapen, A., Poesen, J., Govers, G., Gysels, G., & Nachtergaele, J. (2007). Resistance of soils to concentrated flow erosion: A review. *Earth-Science Reviews*, 80, 75–109. <https://doi.org/10.1016/j.earscirev.2006.08.001>
- Li, Y., Yu, H. Q., Zhou, N., Tian, G., Poesen, J., & Zhang, Z. D. (2015). Linking fine root and understory vegetation to channel erosion in forested hillslopes of southwestern China. *Plant and Soil*, 389, 323–334. <https://doi.org/10.1007/s11104-014-2362-8>
- Li, Z., Zhang, Y., Zhu, Q. K., He, Y. M., & Yao, W. J. (2015). Assessment of bank gully development and vegetation coverage on the Chinese Loess Plateau. *Geomorphology*, 228, 462–469. <https://doi.org/10.1016/j.geomorph.2014.10.005>
- Liu, X. Y., Liu, B., & Yang, S. T. (2014). Driving force of sediment production and potential of sediment reduction in the gullied rolling loess area. *Yellow River*, 36, 1–3. <https://doi.org/10.3969/j.issn.1000-1379.2014.05.001> (in Chinese).
- Makanzu Imwangana, F., Dewitte, O., Ntombi, M., & Moeyersons, J. (2014). Topographic and road control of mega-gullies in Kinshasa (DR Congo). *Geomorphology*, 217, 131–139. <https://doi.org/10.1016/j.geomorph.2014.04.021>
- Martínez-Casasnovas, J. A., Ramos, M. C., & García-Hernández, D. (2009). Effects of land-use changes in vegetation cover and sidewall erosion in a gully head of the Penedès region (northeast Spain). *Earth Surface Processes and Landforms*, 34, 1927–1937. <https://doi.org/10.1002/esp.1870>
- Mhired, D. A., Dagnew, D. C., Alemie, T. C., Guzman, C. D., Tilahun, S. A., Zaitchik, B. F., & Steenhuis, T. S. (2019). Impact of soil conservation and eucalyptus on hydrology and soil loss in the Ethiopian Highlands. *Water*, 11, 2299–2315. <https://doi.org/10.3390/w11112299>
- Moore, J. S. (1997). Field procedures for the headcut erodibility index. *Transactions of the ASAE*, 40, 325–336. <https://doi.org/10.13031/2013.21277>
- Morgan, R. P. C., & Mngomezulu, D. (2003). Threshold conditions for initiation of valley-side gullies in the Middle Veld of Swaziland. *Catena*, 50, 401–414. [https://doi.org/10.1016/S0341-8162\(02\)00129-7](https://doi.org/10.1016/S0341-8162(02)00129-7)
- Mukai, S. (2017). Gully erosion rates and analysis of determining factors: A case-study from the semiarid main Ethiopian Rift Valley. *Land Degradation & Development*, 28, 602–615. <https://doi.org/10.1002/ldr.2532>
- Nachtergaele, J., & Poesen, J. (1999). Assessment of soil losses by ephemeral gully erosion using high-altitude (stereo) aerial photographs. *Earth Surface Processes and Landforms*, 24, 693–706. [https://doi.org/10.1002/\(SICI\)1096-9837\(199908\)24:8<693::AID-ESP992>3.0.CO;2-7](https://doi.org/10.1002/(SICI)1096-9837(199908)24:8<693::AID-ESP992>3.0.CO;2-7)
- Nyssen, J., Poesen, J., Veyret-Picot, M., Moeyersons, J., Haile, M., Deckers, J., ... Govers, G. (2006). Assessment of gully erosion rates through interviews and measurements: A case study from northern Ethiopia. *Earth Surface Processes and Landforms*, 31, 167–185. <https://doi.org/10.1002/esp.1317>
- Oostwoud Wijdenes, D., & Bryan, R. (2001). Gully-head erosion processes on a semi-arid valley floor in Kenya: A case study into temporal variation and sediment budgeting. *Earth Surface Processes and Landforms*, 26, 911–933. <https://doi.org/10.1002/esp.225>
- Oostwoud Wijdenes, D., Poesen, J., Vandekerckhove, L., & Ghesquiere, M. (2000). Spatial distribution of gully head activity and sediment supply along an ephemeral channel in a Mediterranean environment. *Catena*, 39, 147–167. [https://doi.org/10.1016/S0341-8162\(99\)00092-2](https://doi.org/10.1016/S0341-8162(99)00092-2)
- Oostwoud Wijdenes, D., Poesen, J., Vandekerckhove, L., Nachtergaele, J., & De Baerdemaeker, J. (1999). Gully-head morphology and implications for gully development on abandoned fields in a semi-arid environment, Sierra de Gata, southeast Spain. *Earth Surface*

- Processes and Landforms*, 24, 585–603. [https://doi.org/10.1002/\(SICI\)1096-9837\(199907\)24:7<585::AID-ESP976>3.0.CO;2-%23](https://doi.org/10.1002/(SICI)1096-9837(199907)24:7<585::AID-ESP976>3.0.CO;2-%23)
- Poesen, J., Nachtergaele, J., Verstraeten, G., & Valentin, C. (2003). Gully erosion and environmental change: Importance and research needs. *Catena*, 50, 91–133. [https://doi.org/10.1016/S0341-8162\(02\)00143-1](https://doi.org/10.1016/S0341-8162(02)00143-1)
- Poesen, J., Torri, D., & Vanwalleghem, T. (2011). Gully erosion: Procedures to adopt when modelling soil erosion in landscapes affected by gully-ing. In R. Morgan & M. Nearing (Eds.), *Handbook of erosion modelling* (pp. 360–386). Pondicherry, India: Blackwell Publishing Ltd. <https://doi.org/10.1002/9781444328455.ch19>
- Poesen, J., Vandaele, K., & Van Wesemael, B. (1996). Contribution of gully erosion to sediment production in cultivated lands and rangelands. *IAHS-AISH Publication*, 236, 251–266.
- Pollen, N. (2007). Temporal and spatial variability in root reinforcement of streambanks: Accounting for soil shear strength and moisture. *Catena*, 69, 197–205. <https://doi.org/10.1016/j.catena.2006.05.004>
- Qin, C., He, C., Zheng, F. L., Han, L. F., & Zeng, C. S. (2018). Quantitative research of rill head advancing process on loessial hillslope. *Transactions of the Chinese Society of Agricultural Engineering*, 34, 160–167. <https://doi.org/10.11975/j.issn.1002-6819.2018.06.020>
- Rengers, F. K., & Tucker, G. E. (2014). Analysis and modeling of gully head-cut dynamics, North American high plains. *Journal of Geophysical Research: Earth Surface*, 119, 983–1003. <https://doi.org/10.1002/2013JF002962>
- Rieke-Zapp, D. H., & Nichols, M. H. (2011). Headcut retreat in a semiarid watershed in the southwestern United States since 1935. *Catena*, 87, 1–10. <https://doi.org/10.1016/j.catena.2011.04.002>
- Robinson, K. M., & Hanson, G. J. (1996). Gully headcut advance. *Transactions of the ASAE*, 39, 33–38. <https://doi.org/10.13031/2013.27477>
- Samani, A. N., Chen, Q., Khalighi, S., Wasson, R. J., & Rahdari, M. R. (2016). Assessment of land use impact on hydraulic threshold conditions for gully head cut initiation. *Hydrology and Earth System Sciences*, 20, 3005–3012. <https://doi.org/10.5194/hess-20-3005-2016>
- Simon, A., & Collison, A. J. C. (2002). Quantifying the mechanical and hydrologic effects of riparian vegetation on streambank stability. *Earth Surface Processes and Landforms*, 27, 527–546. <https://doi.org/10.1002/esp.325>
- Stein, O. R., & Julien, P. Y. (1993). Criterion delineating the mode of head-cut migration. *Journal of Hydraulic Engineering*, 119, 37–50. [https://doi.org/10.1061/\(ASCE\)0733-9429\(1993\)119:1\(37\)](https://doi.org/10.1061/(ASCE)0733-9429(1993)119:1(37))
- Stein, O. R., Julien, P. Y., & Alonso, C. V. (1993). Mechanics of jet scour downstream of a headcut. *Journal of Hydraulic Research*, 31, 723–738. <https://doi.org/10.1080/00221689309498814>
- Su, Z. A., Xiong, D. H., Dong, Y. F., Li, J. J., Yang, D., Zhang, J. H., & He, G. X. (2014). Simulated headward erosion of bank gullies in the Dry-hot Valley Region of southwest China. *Geomorphology*, 204, 532–541. <https://doi.org/10.1016/j.geomorph.2013.08.033>
- Tebebu, T. Y., Abiy, A. Z., Zegeye, A. D., Dahlke, H. E., Easton, Z. M., Tilahun, S. A., ... Steenhuis, T. S. (2010). Surface and subsurface flow effect on permanent gully formation and upland erosion near Lake Tana in the northern highlands of Ethiopia. *Hydrology and Earth System Sciences*, 7, 5235–5265. <https://doi.org/10.5194/hessd-7-5235-2010>
- Temple, D. M., & Moore, J. S. (1997). Headcut advance prediction for earth spillways. *Transactions of the ASAE*, 40, 557–562. <https://doi.org/10.13031/2013.21314>
- Thompson, J. R. (1964). Quantitative effect of watershed variables on rate of gully head advancement. *Transactions of the ASAE*, 7, 54–55. <https://doi.org/10.13031/2013.40694>
- Torri, D., & Poesen, J. (2014). A review of topographic threshold conditions for gully head development in different environments. *Earth-Science Reviews*, 130, 73–85. <https://doi.org/10.1016/j.earscirev.2013.12.006>
- Torri, D., Poesen, J., Rossi, M., Amici, V., Spennacchi, D., & Cremer, C. (2018). Gully head modelling: A Mediterranean badland case study. *Earth Surface Processes and Landforms*, 43, 2547–2561. <https://doi.org/10.1002/esp.4414>
- Valentin, C., Poesen, J., & Li, Y. (2005). Gully erosion: Impacts, factors and control. *Catena*, 63, 132–153. <https://doi.org/10.1016/j.catena.2005.06.001>
- Vandekerckhove, L., Poesen, J., & Govers, G. (2003). Medium-term gully headcut retreat rates in Southeast Spain determined from aerial photographs and ground measurements. *Catena*, 50, 329–352. [https://doi.org/10.1016/S0341-8162\(02\)00132-7](https://doi.org/10.1016/S0341-8162(02)00132-7)
- Vandekerckhove, L., Poesen, J., Oostwoud Wijdenes, D., & Gyssels, G. (2001). Short-term bank gully retreat rates in Mediterranean environments. *Catena*, 44, 133–161. [https://doi.org/10.1016/S0341-8162\(00\)00152-1](https://doi.org/10.1016/S0341-8162(00)00152-1)
- Vandekerckhove, L., Poesen, J., Oostwoud Wijdenes, D., Nachtergaele, J., Kosmas, C., Roxo, M. J., & Figueiredo, T. D. (2000). Thresholds for gully initiation and sedimentation in Mediterranean Europe. *Earth Surface Processes and Landforms*, 25, 1201–1220. [https://doi.org/10.1002/1096-9837\(200010\)25:113.O.CO;2-L](https://doi.org/10.1002/1096-9837(200010)25:113.O.CO;2-L)
- Vanmaercke, M., Poesen, J., Van Mele, B., Demuzere, M., Bruynseels, A., Golosov, V., ... Yermolaev, O. (2016). How fast do gully headcuts retreat? *Earth-Science Reviews*, 154, 336–355. <https://doi.org/10.1016/j.earscirev.2016.01.009>
- Vannoppen, W., Vanmaercke, M., Baets, S. D., & Poesen, J. (2015). A review of the mechanical effects of plant roots on concentrated flow erosion rates. *Earth-Science Reviews*, 150, 666–678. <https://doi.org/10.1016/j.earscirev.2015.08.011>
- Vanwalleghem, T., Poesen, J., Nachtergaele, J., & Verstraeten, G. (2005). Characteristics, controlling factors and importance of deep gullies under cropland on loess-derived soils. *Geomorphology*, 69, 76–91. <https://doi.org/10.1016/j.geomorph.2004.12.003>
- Wang, X., Zhong, X., Liu, S., & Li, M. H. (2008). A non-linear technique based on fractal method for describing gully-head changes associated with land-use in an arid environment in China. *Catena*, 72, 106–112. <https://doi.org/10.1016/j.catena.2007.04.007>
- Xing, T., Li, Z., Liu, P. L., Jia, X. A., & Liu, Y. (1991). Survey and evaluation of disaster caused by heavy rainstorm occurred on July 23, 1988 and water and soil conservation measures in Xifeng Area, Gansu Province. *Bulletin of Soil and Water Conservation*, 11, 40–47. <https://doi.org/10.13961/j.cnki.stbctb.1991.03.009> (in Chinese).
- Xu, X. M., Wilson, G. V., Zheng, F. L., & Tang, Q. H. (2020). The role of soil pipe and pipeflow in headcut migration processes in loessic soils. *Earth Surface Processes and Landforms*, 45, 1749–1763. <https://doi.org/10.1002/esp.4843>
- Xu, X. Z., Liu, Z. Y., Wang, W. L., Zhang, H. W., Yan, Q., Zhao, C., & Guo, W. Z. (2015). Which is more hazardous: Avalanche, landslide, or mudslide? *Natural Hazards*, 76, 1939–1945. <https://doi.org/10.1007/s11069-014-1570-0>
- Xu, X. Z., Zhang, H. W., Wang, W. L., Zhao, C., & Yan, Q. (2015). Quantitative monitoring of gravity erosion using a novel 3D surface measuring technique: Validation and case study. *Natural Hazards*, 75, 1927–1939. <https://doi.org/10.1007/s11069-014-1405-z>
- Yan, Y., Zhang, X. Y., Liu, J. L., Li, J. Y., Ding, C., Shen, Q. S., & Guo, M. M. (2020). The effectiveness of selected vegetation communities in regulating runoff and soil loss of regraded gully banks in the Mollisol region of Northeast China. *Land Degradation & Development*. <https://doi.org/10.1002/ldr.3866>
- Yang, L. S., Li, C. B., Wang, S. B., & Yang, W. J. (2014). Water balance within soil water reservoir in the loess tableland by means of combination of SWAT model and remote sensing: A case study in the Dongzhi Loess Tableland of eastern Gansu. *Journal of Glaciology and Geocryology*, 36, 691–698. <https://doi.org/10.7522/j.issn.1000-0240.2014.0083> (in Chinese).
- Yu, G. Q., Zhang, X., Zhang, M. S., & Pei, L. (2012). Mechanism of vegetation regulating on gravitational erosion in the slope-gully system on

- the Loess Plateau. *Journal of Natural Resources*, 27, 922–932. <https://doi.org/10.11849/zrzyxb.2012.06.004> (in Chinese).
- Zegeye, A. D., Langendoen, E. J., Steenhuis, T. S., Mekuria, W., & Tilahun, S. A. (2020). Bank stability and toe erosion model as a decision tool for gully bank stabilization in sub-humid Ethiopian Highlands. *Ecohydrology and Hydrobiology*, 20, 301–311. <https://doi.org/10.1016/j.ecohyd.2020.02.003>
- Zegeye, A. D., Langendoen, E. J., Tilahun, S. A., Mekuria, W., Poesen, J., & Steenhuis, T. S. (2018). Root reinforcement to soils provided by common Ethiopian Highlands plants for gully erosion control. *Ecohydrology*, 11, e1940. <https://doi.org/10.1002/eco.1940>
- Zegeye, A. D., Steenhuis, T. S., Mekuria, W., Dagnaw, D. C., Addisse, M. B., Tilahun, S. A., & Kasse, T. A. (2017). Effect of gully headcut treatment on sediment load and gully expansion in the sub humid Ethiopian Highlands. *Environment & Ecology Research*, 5, 138–144. <https://doi.org/10.13189/eer.2017.050208>
- Zhang, B. J., Xiong, D. H., Zhang, G. H., Wu, H., Zhang, S., Yuan, Y., & Dong, Y. F. (2018). Simulation and verification of overhanging soil layers stability of gully heads in Yuanmou dry-hot valley based on moment method. *Transactions of the Chinese Society of Agricultural Engineering*, 34, 133–140. <https://doi.org/10.11975/j.issn.1002-6819.2018.15.017> (in Chinese).
- Zhang, B. J., Xiong, D. H., Zhang, G. H., Zhang, S., Wu, H., Yang, D., ... Lu, X. N. (2018). Impacts of headcut height on flow energy, sediment yield and surface landform during bank gully erosion processes in the Yuanmou dry-hot valley region, southwest China. *Earth Surface Processes and Landforms*, 43, 2271–2282. <https://doi.org/10.1002/esp.4388>
- Zhang, H. X. (1983). The characteristics of hard rain and its distribution over the Loess Plateau. *Acta Geographica Sinica*, 38, 416–425 (in Chinese).
- Zhang, R. J., Guo, J., Yu, Y. L., Zhang, X. N., Zuo, R., & Hu, W. F. (2015). Study on benefit of water diversion and soil conservation for water and soil conservation in gullied loess plateaus. *Yellow River*, 37, 98–101+108. <https://doi.org/10.3969/j.issn.1000-1379.2015.04.024> (in Chinese).
- Zheng, F. L., Xu, X. M., & Qin, C. (2016). A review of gully erosion process research. *Transactions of the Chinese Society for Agricultural Machinery*, 47, 48–59+116. <https://doi.org/10.6041/j.issn.1000-1298.2016.08.008> (in Chinese).

SUPPORTING INFORMATION

Additional supporting information may be found online in the Supporting Information section at the end of this article.

How to cite this article: Kang H, Wang W, Guo M, Li J, Shi Q. How does land use/cover influence gully head retreat rates? An in-situ simulation experiment of rainfall and upstream inflow in the gullied loess region, China. *Land Degrad Dev.* 2021;32:2789–2804. <https://doi.org/10.1002/ldr.3892>